Full Length Article

# A new model for permeability impairment due to asphaltene deposition

Davud Davudov*, Rouzbeh Ghanbarnezhad Moghanloo

*The University of Oklahoma, United States*

ABSTRACT

The existing theoretical and empirical models to describe asphaltene deposition in porous media do not consider the complicated structure of pore network. Permeability reduction due to asphaltene deposition has been mainly attributed to pore volume shrinkage (porosity reduction). However, asphaltene particles can also block pore throats which will lead to severe permeability reduction even when a large fraction of total pore volume still remains intact. Thus, there is a need for permeability models that are explicitly function of pore/hydraulic connectivity. This paper provides a review of the existing models and examines a permeability model that explain permeability impairment due to asphaltene deposition.

In this study, we propose a new permeability model based on Critical Path Analysis (CPA) which is a function of average coordination number (average number of available/connected neighbor pores). Furthermore, experimental data in the literature related to limestone, sandstone and carbonate (dolomite) samples are utilized to understand combined effects of surface deposition and interconnectivity loss due to pore blockage on permeability reduction.

We observed that surface deposition is the dominant mechanism in the limestone samples studied here owing to large pore throat size compared to the particle size. In the sandstone samples, both the surface deposition and pore throat plugging mechanisms contribute fairly the same in the observed permeability reduction. For the carbonate (dolomite) samples, the pore blockage is the dominant mechanism, which results in rapid sharp decrease of the permeability. It is expected that the outcome of this work improves prediction of the asphaltene deposition in the near wellbore region.

## 1. Introduction

The issue of asphaltene deposition has plagued the oil and gas industry for decades since it has been identified and named as "asphaltenes" in 1837 [7]. Due to the huge costs associated with remediation, it is extremely important to understand the issue of asphaltene deposition and the factors affecting it [14]. Crude oil has several fractions, and asphaltenes essentially tend to be its heaviest, polarizable fractions. They are known as the "cholesterol of petroleum" due to their ability to precipitate as solids and subsequently deposit with changing pressure, temperature and oil composition [3]. Asphaltene precipitation is called the process when asphaltenes become a separate phase from the crude oil. They remain suspended in the liquid phase where the quantity and the size of the asphaltenes are relatively small. The precipitated asphaltenes clump together (aggregation) and form larger particles, also called flocs. The asphaltene aggregates are initially suspended in the crude oil. Subsequently, the flocs may attach to and accumulate on various surfaces, a process which is called asphaltene deposition [28]. In both up and downstream operations deposition may cause severe

problems. Asphaltenes may precipitate and deposit on surface of pipelines, bottom of distillation column and heat exchangers as well, affecting efficiency and creating added economic costs to remediate [18,10].

Also, during production, asphaltene particles can deposit in reservoir, leading to possible blocking of flow, particularly in the near wellbore region. Asphaltene deposition problems encountered deep down in rock reservoirs are extremely problematic, and very challenging to tackle, as opposed to production tubing deposition problems. Minssieux [22] studied various core samples with different rock characteristics in core-flooding experiments, with regards to porous media. He concluded that porous sample plugging only seemed to occur after enough oil had flown through the sample, and that damage at earlier times was only observed in samples with a lower initial permeability [28].

The mechanisms through which formation damage due to asphaltene deposition can occur are surface deposition, and pore throat plugging. As asphaltene deposits accumulate on the pore surface, the pore surface area decreases leading to porosity reduction. Moreover,

when asphaltene deposits accumulate in front of a pore, they can plug them causing severe permeability reduction.

For modeling of permeability impairment in porous media due to asphaltene deposition, Deep Bed Filtration (DBF) models are often used [31,4]. Using DBF theory, Wang [31] modified Civan's model for near wellbore asphaltene deposition, assuming negligible capillary pressure and one dimensional horizontal flow:

$$\frac{\partial E_A}{\partial t} = \alpha C_A \phi - \beta E_A (v_L - v_{cr,L}) + \gamma u_L C_A \qquad (1)$$

where, $E_A$ is volume fraction of deposition asphaltenes; $v_L$ is interstitial velocity $(=u_L/\phi)$; $v_{cr,L}$ is critical interstitial velocity; $u_L$ is superficial velocity; $\alpha$ is surface deposition rate coefficient; $\beta$ is entrainment rate coefficient; $\gamma$ is pore throat plugging coefficient. The first term in Eq. (1) represents the pore surface deposition rate which is directly proportional to the concentration of suspended particle concentration in the flowing fluid; the second term expresses the entrainment of asphaltene particles (removal due to drag force) that becomes dominant above critical interstitial velocity [8]; and the last term describes for the pore throat plugging rate, where the plugging rate is directly proportional to the superficial velocity. Wang [31] defined the pore plugging coefficient, $\gamma$ as:

$$\gamma = \gamma_i (1 + \sigma E_a), \ if \ 0 > R > R_c$$
$$\gamma = 0, \ otherwise \qquad (2)$$

where, $\sigma$ is deposition constant; $R$ refers to the ratio of particle size to pore throat size, $R_c$ refers to the critical ratio of particle size to pore throat size. According to Eq. (2) ore throat plugging occurs at conditions where critical pore throat diameter is greater than the average pore throat diameter.

Boek et al [4] discussed that DBF models are very simplistic. Thus, using stochastic rotation dynamics models in capillary flow, Boek et al. [4] estimated coefficients needed for DBF deposition model at the Darcy-scale. They have suggested that experimental deposition data can be modeled using only surface deposition rate, $(\alpha)$ parameter obtained from straight capillary model. However, their model still neglects the effect of pore blockage on permeability reduction.

Asphaltene deposition can lead to porosity and permeability reduction; however, in the majority of existing models, permeability reduction is only attributed to pore volume shrinkage (porosity reduction). Local dynamic porosity is computed as the difference between the original porosity, $\phi_i$, and the fraction of asphaltene deposits, ε:

$$\phi = \phi_i - \varepsilon \qquad (3)$$

Further, permeability change as a function of porosity is estimated as a function of porosity reduction [32,21]:

$$\frac{k}{k_i} = \left(\frac{\phi}{\phi_i}\right)^3 \qquad (4)$$

However, in Eq. (4) connectivity loss (pore connectivity) has not been considered and permeability reduction is only attributed to pore volume reduction. It is well known that effective porosity can decrease owing to pore volume shrinkage and thus permeability can be reduced. However, permeability can be also altered because of hydraulic conductivity/connectivity loss (coordination number reduction) owing to pore plugging mechanism (Fig. 1). In the extreme cases where significant pore blockage occurs, total pore volume may not even greatly change. As it will be discussed later in detail, when the rock sample has a large fraction of pores with the diameter comparable to the size of particles, pore throats can be easily plugged and blocked; this will lead to severe permeability reduction even when the large fraction of pore space yet remains intact. Thus, it is crucial to study asphaltene deposition in porous media via permeability models which consider both porosity reduction and pore connectivity loss, especially for reservoirs with small size pores that are comparable to the particle size.
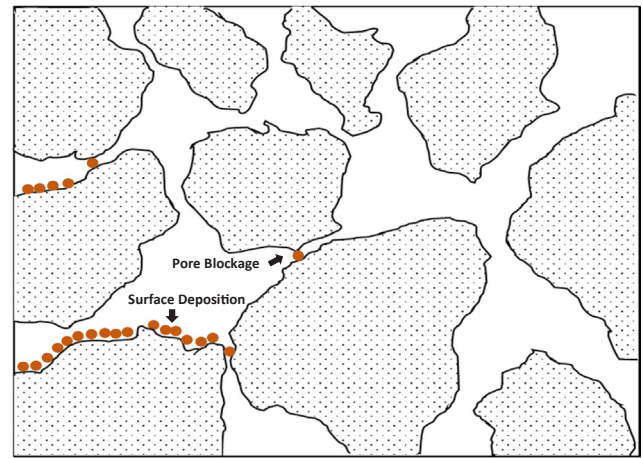


**Fig. 1.** Schematic of permeability reduction due to surface deposition and pore plugging.

**Table 1**
Initial parameters of samples.

| Sample # | Asphaltene wt% | Initial Porosity, % | Initial Permeability, md | Initial Coordination Number, z |
|---|---|---|---|---|
| Limestone #1 | 6.56 | 48.54 | 1062.5 | 8.5 |
| Limestone #2 | 16.3 | 22.5 | 106.6 | 6.4 |
| Sandstone #1 | 6.56 | 49.16 | 1089.6 | 8.5 |
| Sandstone #2 | 16.3 | 13.5 | 22.8 | 4.9 |
| Sandstone #3 | 12.94 | 16.0 | 66.3 | 5.4 |
| Carbonate #1 | 0.06 | 17.17 | 4.67 | 5.6 |
| Carbonate #2 | 0.87 | 21.2 | 6.32 | 6.2 |
| Carbonate #3 | 1.5 | 19.24 | 5.48 | 5.9 |

In this study, we develop a permeability model based on Critical Path Analysis (CPA) that is a function of average coordination number (average number of available/connected neighbor pores). Furthermore, experimental data in the literature related to limestone, sandstone and carbonate (dolomite) samples are utilized to understand combined effects of surface deposition and interconnectivity loss due to pore blockage on permeability reduction.

## 2. Permeability model

The interplay between porosity/storage and permeability/hydraulic conductivity has been studied for decades. As a result, many theoretical models have been developed to estimate hydraulic conductivity of porous media [12,6], Bernabé et al. [2]. One of the fundamental permeability models is Kozeny-Carmen (KC) equation that considers porous medium as a bundle of cylindrical tubes:

$$k = \frac{1}{c} \frac{\phi}{\tau} \frac{1}{S_{gv}} \left(\frac{\phi}{1-\phi}\right)^2, \qquad (5)$$

However, Civan [5] suggested that KC equation cannot properly address the gate/valve effect of porous media (pore/hydraulic connectivity) to predict permeability when pore throats are blocked and isolated. Therefore, he modified KC model by including interconnectivity parameter, Γ:

$$k = \Gamma \phi \left(\frac{\phi}{1-\phi}\right)^{2\beta}, \qquad (6)$$

Γ is a measure of the pore space connectivity, and it represents the valve effect of the pore throats controlling the pore connectivity to other pore spaces [6]. the interconnectivity parameter is strong function of average coordination number, z (the number of the pore throats)
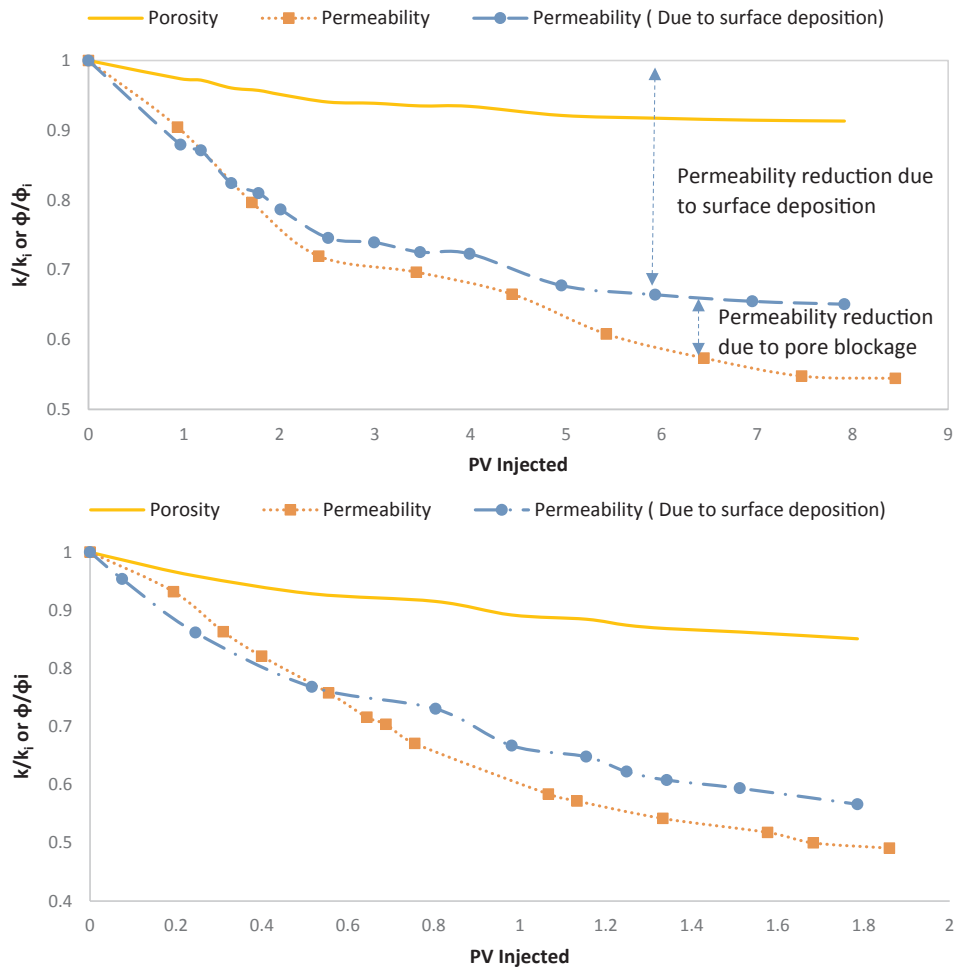
**Fig. 2.** Impact of surface deposition and pore blockage on permeability reduction for (a) limestone #1 (b) limestone #2 (Experimental data is obtained from [24,2]).

and it becomes zero when all the pore throats are blocked due to mechanisms like fine migration, deposition of precipitates including gels, wax, and asphaltene, and collapse of pore throats under mechanical stresses.

### 2.1. CPA based model

Although models developed based on the premise of bundle of capillary tubes are widely-used, they are not sophisticated enough to represent complicated structure of porous media. Thus, percolation-based models were developed to address issues associated with bundle of capillary tube hypothesis. Sahimi [27] and Hunt [17] reported that pore size in naturally occurring porous media complies with fractal geometry/scaling and that implementing fractal geometry yields successful prediction of permeability. Katz and Thompson [19,20] model was one of the earliest attempts to implement percolation theory based critical path analysis to determine permeability. They have discussed that fluid flow and electrical conductance through porous media are percolation processes, and permeability can be related to electrical conductivity and critical pore throat radius, ($r_c$):

$$k = \frac{1}{c}\frac{\sigma_b}{\sigma_w}r_c^2 = \frac{r_c^2}{c}\frac{1}{F}, \tag{7}$$

where $\sigma_b$ is bulk electrical conductivity, $\sigma_w$ is saturating fluid electrical conductivity, and c is a constant. Here $r_c$ is the critical pore throat radius, defined as the largest value of $r$, for which an interconnected path may exist from one side of a system to the other. Katz and Thompson [19] argued that critical pore radius can be estimated from mercury

intrusion porosimetry data and the inflection point on the mercury intrusion curve corresponds to this critical pore radius.

Following Daigle [9] and Davudov and Moghanloo [11], critical pore radius can be expressed in terms of percolation threshold:

$$r_c = r_{max}(1-p_c)^{\frac{1}{3-D}}, \tag{8}$$

where $r_{max}$ is maximum accessible pore radius, D is fractal dimension, and $p_c$ is critical percolation threshold.

Additionally, formation factor, $F$ which is ratio of electrical conductivity to the electrical conductivity of fluid saturating pore, also may be expressed in terms of total porosity and percolation threshold as [13]:

$$\frac{1}{F} = \left[\frac{\phi(1-p_c)}{1-\phi p_c}\right]^m, \tag{9}$$

Combining Eqs. (7)–(9), Daigle [9] expressed permeability as:

$$k = \frac{r_{max}^2}{c}\left(\frac{\phi}{1-\phi p_c}\right)^m (1-p_c)^{\frac{2}{3-D}+m}, \tag{10}$$

Critical percolation threshold, $p_c$ can be expressed in terms of coordination number as $p_c = 1.5/z$, thus Eq. (10) can be rewritten:

$$k = \frac{r_{max}^2}{c}\phi^m\left(\frac{z}{z-1.5\phi}\right)^m\left(1-\frac{1.5}{z}\right)^{\frac{2}{3-D}+m}, \tag{11}$$

Further, assuming $1-\phi p_c \approx 1$ [26], Eq. (11) can be simplified as:
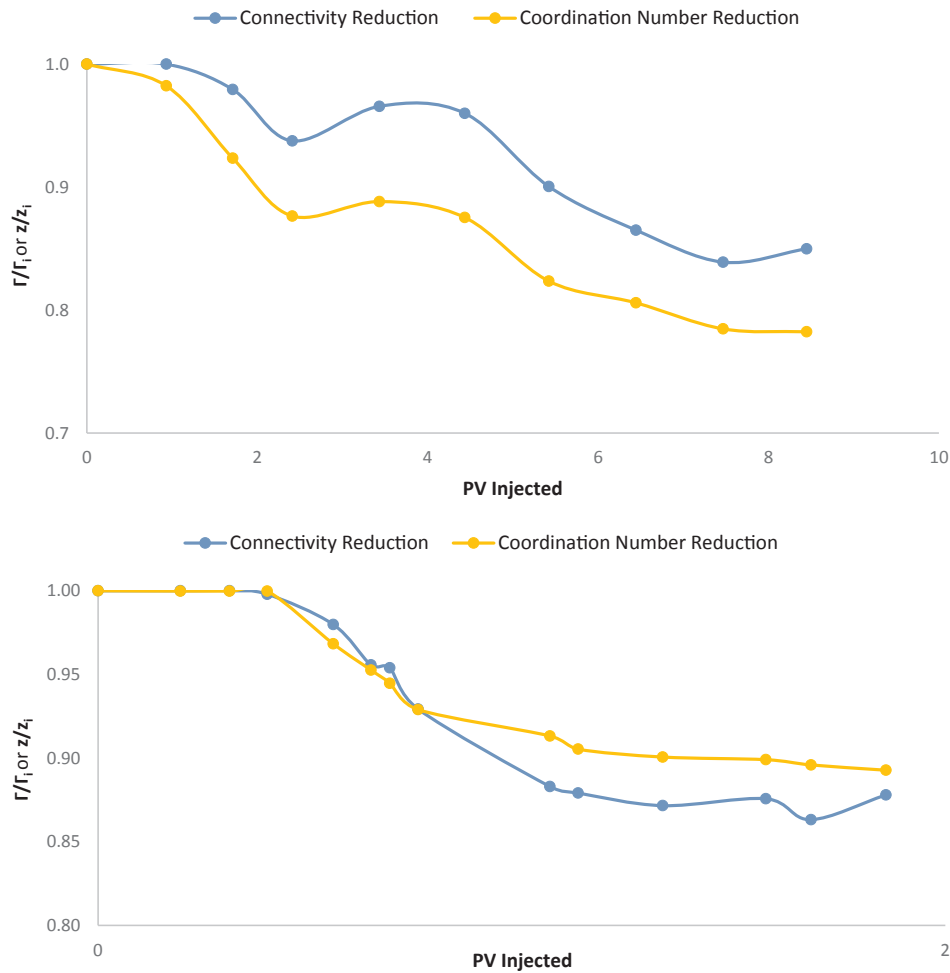
Fig. 3. Interconnectivity ratio and coordination number reduction for (a) limestone #1 (b) limestone #2.

$$k = \frac{r_{\max}^2}{8} \phi^m \left(1 - \frac{1.5}{z}\right)^{\frac{2}{3-D}+m} \tag{12}$$

when Eq. (12) is compared with Civan's model (Eq. (6), it is clear that $r_{max}^2 \phi^2/8$ is maximum achievable permeability where $(1-1.5/z)^{\frac{2}{3-D}+m}$ represents interconnectivity term ($\Gamma$). As coordination number, z gets close to 1.5, permeability will approximate to zero, because of closing valve effect.

## 3. Permeability reduction – effect of surface deposition and pore blockage

The effects of both pore volume shrinkage due to surface deposition and connectivity loss due to pore plugging on permeability reduction can be analyzed based on Civan's permeability model described (Eq. (6)), considering $\beta$ to be unity:

$$\underbrace{\frac{k}{k_i}}_{\text{Total Permeability Reduction}} = \pi \underbrace{\frac{\frac{\phi^3}{(1-\phi)^2}}{\frac{\phi_i^3}{(1-\phi_i)^2}}}_{\text{Surface Deposition}} * \underbrace{\frac{\Gamma}{\Gamma_i}}_{\text{Pore Plugging}} \tag{13}$$

where first and second terms on the right side of Eq. (13) express permeability reduction owing to surface deposition and pore plugging, respectively If pore blockage is insignificant, then surface deposition will be the only mechanism contributing to porosity and permeability reduction can be simplified as:

$$\frac{k}{k_i} = \frac{\frac{\phi^3}{(1-\phi)^2}}{\frac{\phi_i^3}{(1-\phi_i)^2}} \tag{14}$$

Alternatively, assuming $r_{max}^2/r_{\max\_i}^2 = \phi/\phi_i$, permeability reduction from Eq. (11) can be expressed as:

$$\frac{k}{k_i} = \left(\frac{\phi}{\phi_i}\right)^{m+1} \left(\frac{1-\frac{1.5\phi_i}{z_i}}{1-\frac{1.5\phi}{z}}\right)^m \frac{\left(1-\frac{1.5}{z}\right)^{\frac{2}{3-D}+m}}{\left(1-\frac{1.5}{z_i}\right)^{\frac{2}{3-D}+m}} \tag{15}$$

where $z_i$ is initial coordination number and it can be estimated as a function of initial porosity [12,2]:

$$z_i = A + B\log(\phi), \tag{16}$$

where both A and B are constants. Bernabe et al. [3] suggested that for two-dimensional system A is 10.4 and B is equal to 6.25.

In case $1-\phi p_c \approx 1$ [26], Eq. (15) will be simplified as:

$$\frac{k}{k_i} = \left(\frac{\phi}{\phi_i}\right)^{m+1} \frac{\left(1-\frac{1.5}{z}\right)^{\frac{2}{3-D}+m}}{\left(1-\frac{1.5}{z_i}\right)^{\frac{2}{3-D}+m}} \tag{17}$$

## 4. Case studies – evaluation of surface deposition and pore plugging effects

To further illustrate impact of surface deposition and pore plugging effects on permeability reduction, several experimental data sets
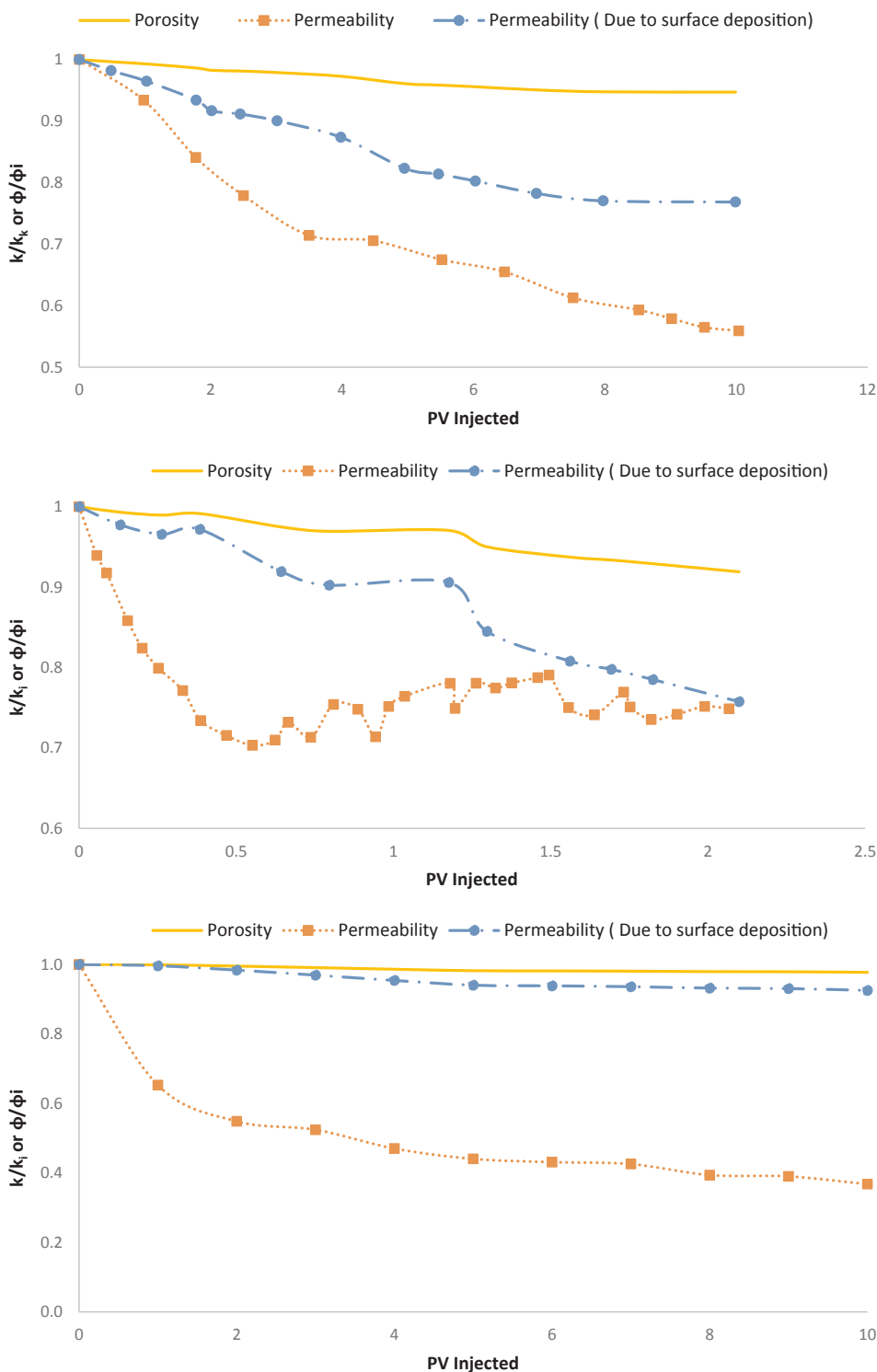
**Fig. 4.** Impact of surface deposition and pore blockage on permeability reduction for (a) sandstone #1 (b) sandstone #2 (c) sandstone #3 (Experimental data is obtained from [24,1,16]).

obtained from limestone, sandstone and carbonate (dolomite) core samples are evaluated here. In these experiments, asphaltene deposition was assessed through pressure drop measurements across the vessel. The amount of deposited asphaltenes within the core was evaluated through the difference of asphaltene content in the inlet and outlet stream. Using the experimental data sets, both initial porosity as well as the damaged/reduced porosity are calculated by subtracting total volume of deposited asphaltene from initial pore volume of the core sample. Initial sample properties and estimated average coordination

number values (Eq. (16) for these samples are listed in Table 1.

Next, permeability reduction as a function of total injected pore volume is calculated for the same experimental data sets. As expected, both porosity reduction and permeability damage are a function pore volume injected (PVI); the larger injected volume, the more reduction in both permeability and porosity is realized.

Since porosity reduction as a function of injected pore volume is known (from experimental data), permeability reduction due to surface deposition can be estimated using Eq. (14) and the ratio between
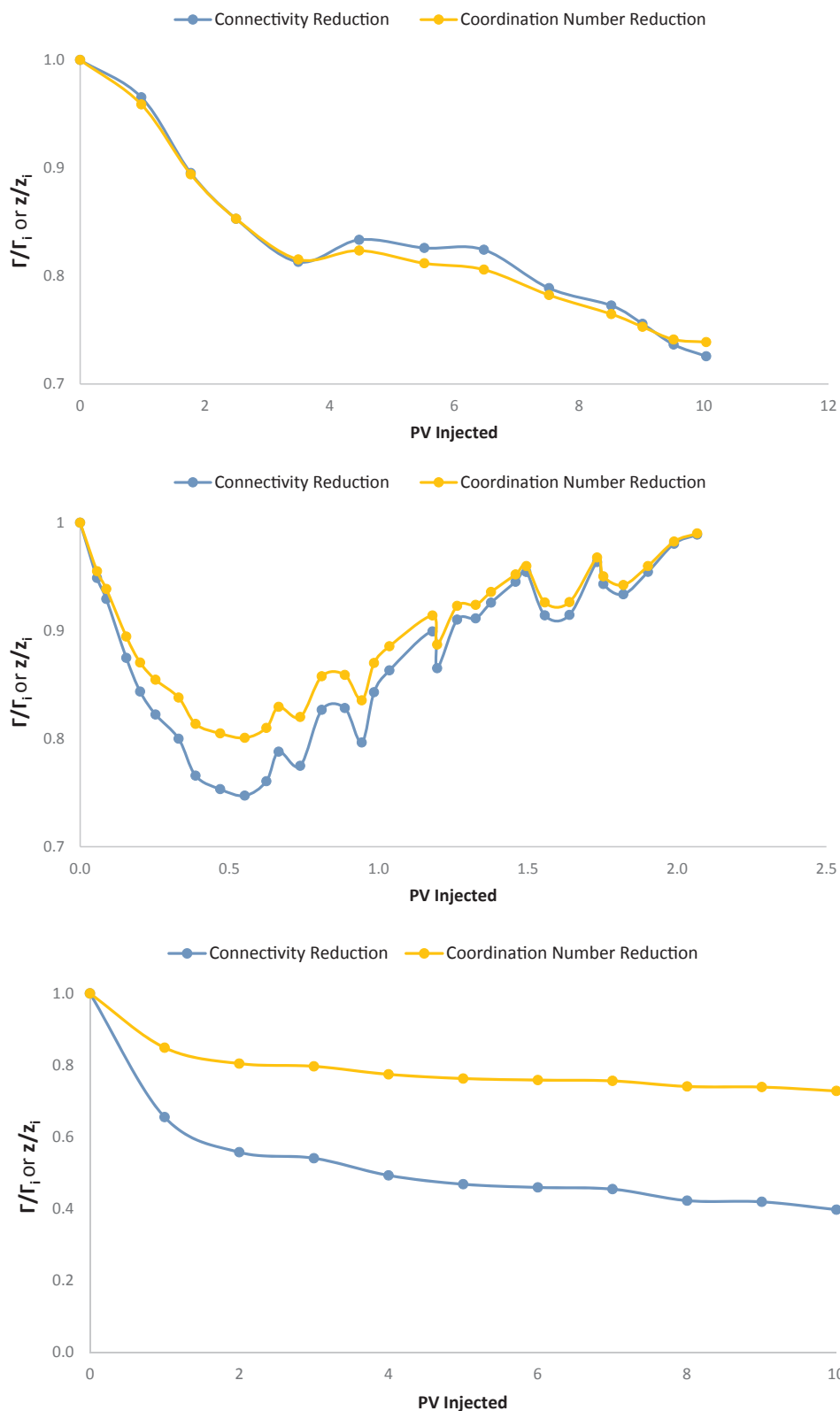
**Fig. 5.** Interconnectivity ratio and coordination number reduction for (a) sandstone #1 (b) sandstone #2 (c) sandstone #3.

predicted and actual permeability values measured in the dataset (Eq. (13) can be attributed to the pore connectivity loss. Moreover, average coordination number reduction can be estimated from Eq. (15) for samples with high initial porosity and from Eq. (17) for samples with low initial porosity.

### 4.1. Limestone samples

The experimentally measured porosity and permeability reduction (as a function of increased effective stress) for limestone samples are compared with the predicted permeability ratio values solely due to surface deposition (Eq. (14) as shown in Fig. 2. As observed in both
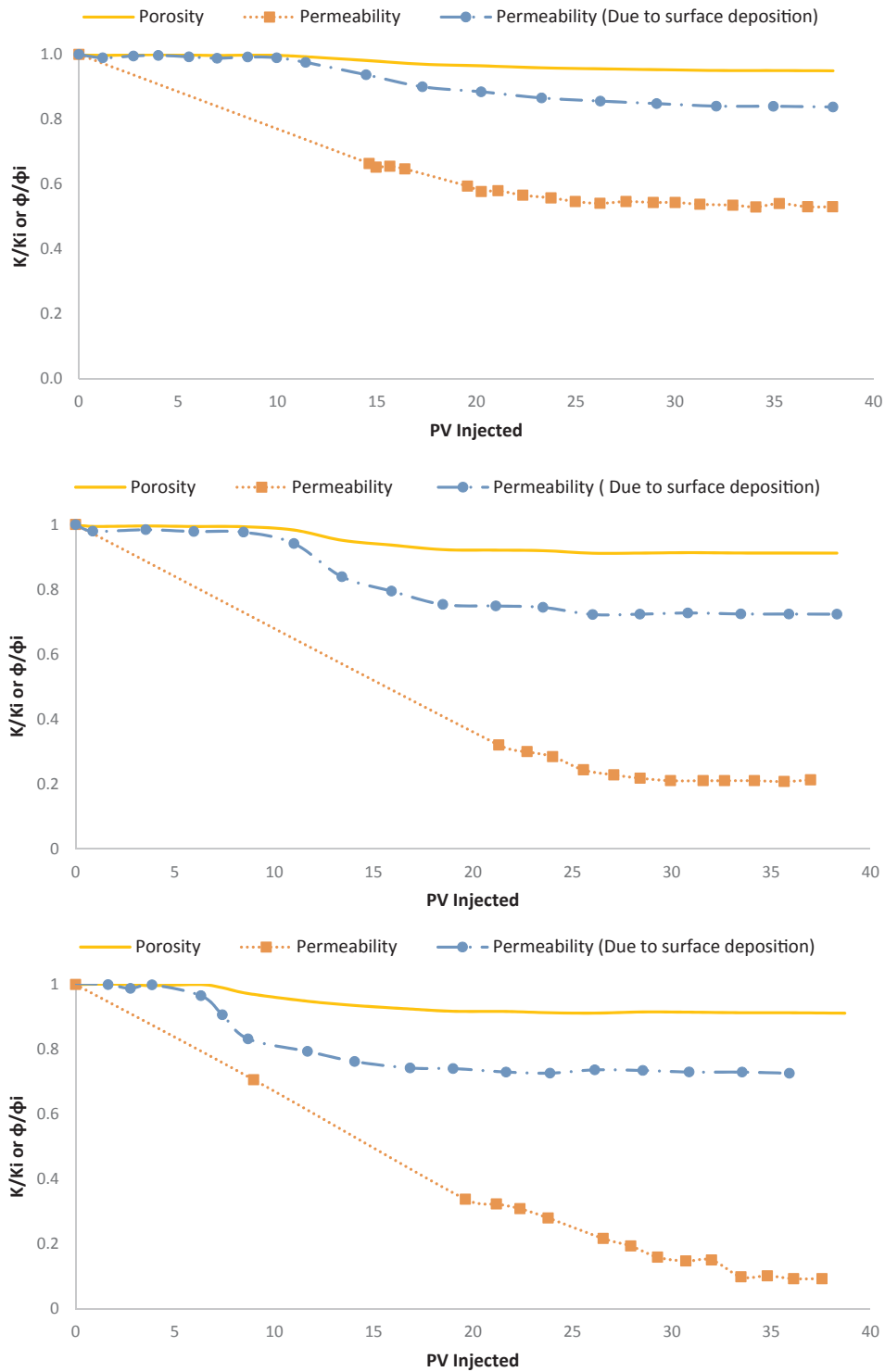
**Fig. 6.** Impact of surface deposition and pore blockage on permeability reduction for (a) carbonate #1 (b) carbonate #2 (c) carbonate #3 (Experimental data is obtained from [29]).

samples, permeability has been reduced around 50% and predicted values from Eq. (14) are close to the measured data. This clearly suggests that, permeability reduction in limestone samples can be predicted solely to the pore volume shrinkage.

Interconnectivity ratio based on Eq. (13) and coordination number reduction based on Eq. (15) are estimated as illustrated in Fig. 3. Results show that connectivity loss for both limestone samples are in the range of 12–15%. Moreover, coordination number reduces from its initial value of 8.5 to 6.65 (22% reduction) for limestone #1 and from

6.4 to 5.7 (11% reduction) for limestone #2, which it can be easily concluded that for limestone samples, major damage mechanism is surface deposition and pore blockage effect is minor.

### 4.2. Sandstone samples

For the sandstone samples studied here, our results indicate that permeability reduction is in the range of 45% for first sample, 30% for second sample and 63% for the last sample (Fig. 4), where connectivity
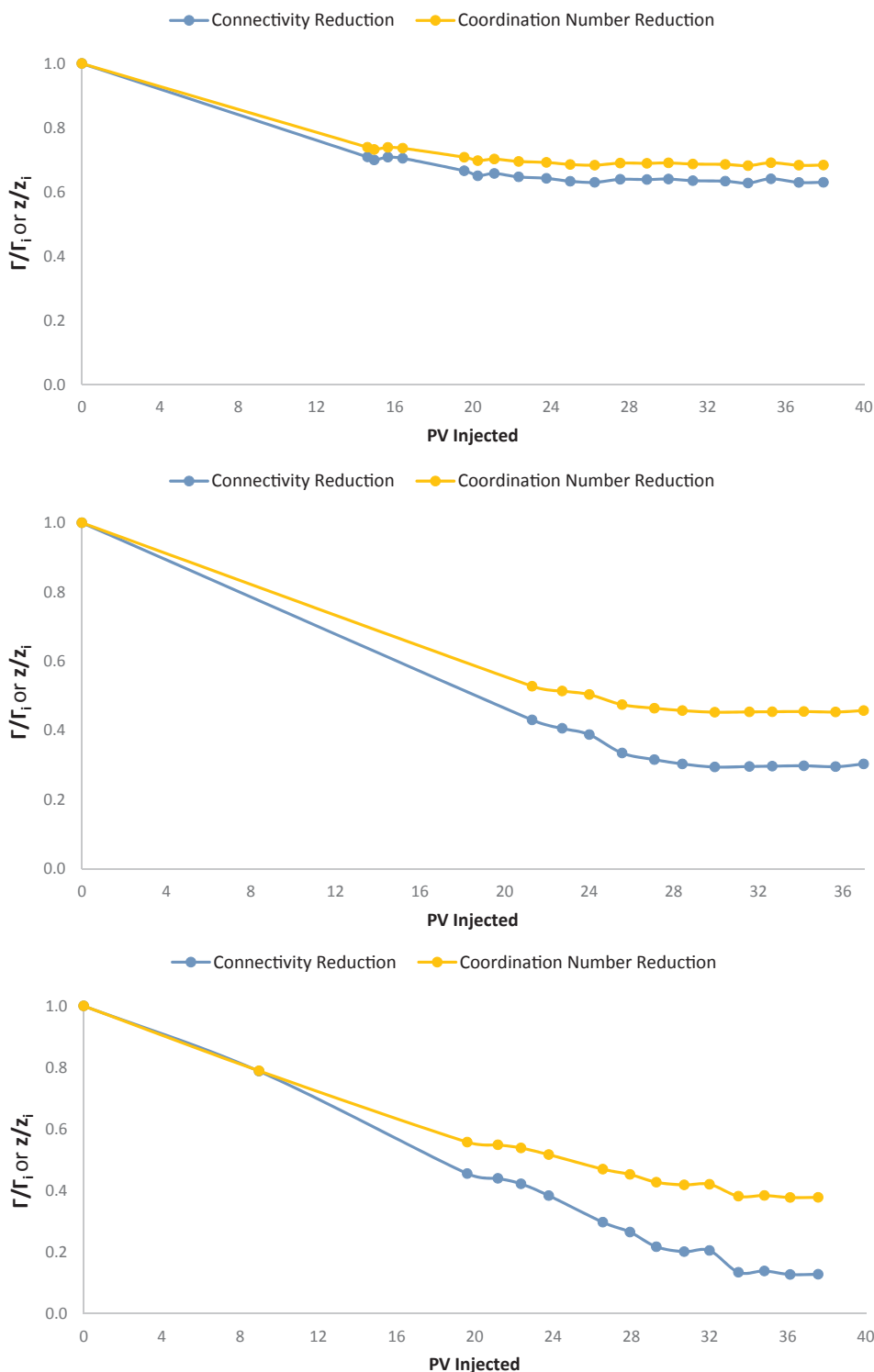
**Fig. 7.** Interconnectivity ratio and coordination number reduction for (a) carbonate #1 (b) carbonate #2 (c) carbonate #3.

loss is around 27%, 25%, and 60% respectively (Fig. 5). Moreover, coordination number for sandstone #1 reduces from 8.5 to 6.3 (26% reduction), for sandstone #2 it reduces from 4.9 to 3.9 (20% reduction) and for sandstone #3 it reduces from 5.4 to 4 (27% reduction). Thus, it is can be concluded that for sandstone samples used in this study, the surface deposition mechanism and pore blockage mechanism have comparable contributions on the permeability reduction. Moreover, for one of the sandstone samples (sample #2), connectivity loss is re-covered after initial decline (Fig. 5. This recovery might be due to

increased injection pressure (possibly to maintain a constant injection rate) which yields sufficient drag force to remove previously deposited particles [21].

### 4.3. Carbonate samples

For carbonate samples studied here, our results suggest that the permeability reduction is sharper than pure limestone and sandstone rock samples whereas porosity change is small Fig. 6). Results indicate
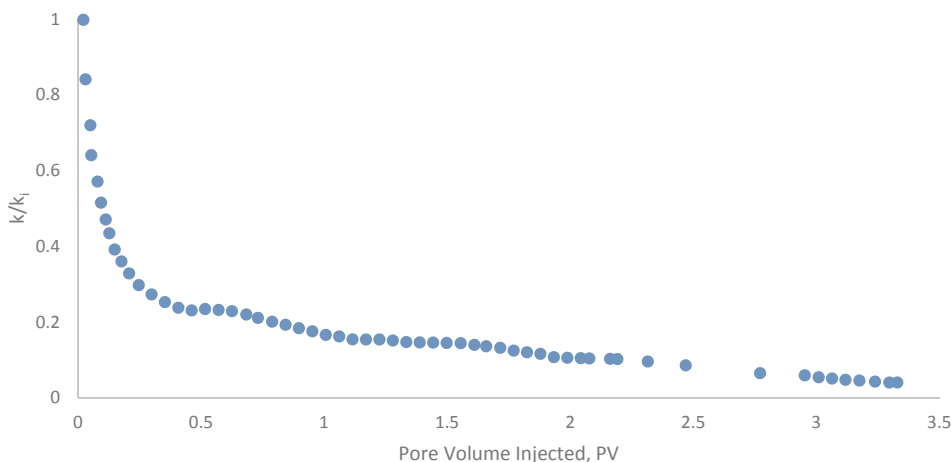
**Fig. 8.** Permeability reduction as a function of injected PV for carbonate sample (Experimental data is obtained from [21]).
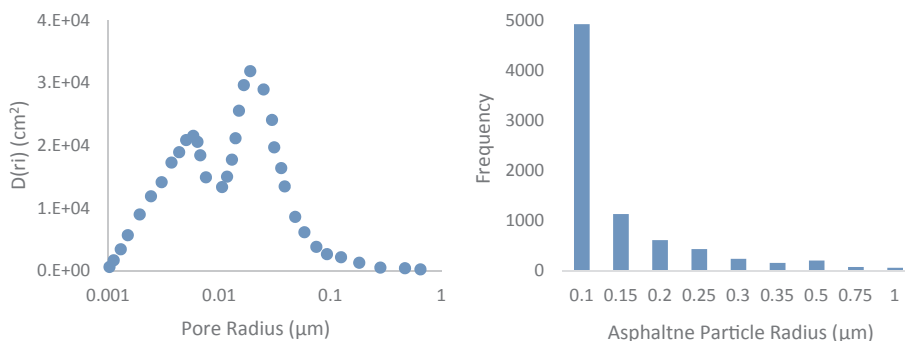


**Fig. 9.** (a) Pore size distribution and (b) Particle size distribution (Data is obtained from [21]).
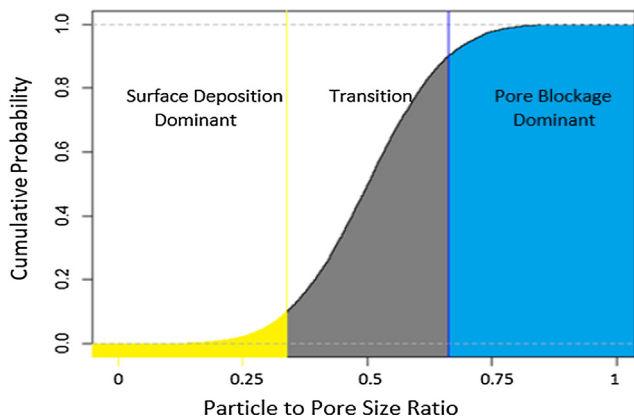


**Fig. 10.** Generic cumulative density distribution for particle to pore size ratio.

that, the contribution of pore throat plugging mechanism on permeability reduction is in the range of 37% for first sample, where this value is around 70% and 88% for second and third samples and, co-ordination number reduces to 32%, 55% and 63% respectively (Fig. 7).

One of the major reasons for severe connectivity loss in carbonate samples is that for low permeability formations, pore size diameter is relatively small, and thus pore plugging becomes dominant. The pore plugging mechanism leads to steeper decline in permeability leaving the large fraction of pore space intact. Moreover, existence of polar groups on the inner surface of carbonate samples makes the asphaltene molecules adhere more strongly to the rock surface, and hence increases asphaltene deposition [15,1].

The results of this study are consistent with Nasri and Dabir [25] study, where they did network modelling analysis on asphaltene

deposition in carbonates, and they mentioned that the main reason of absolute permeability reduction in carbonate samples is plugging of the pore throats.

Moreover, Shen and Sheng [30] have reported that asphaltene deposition may have a tremendous impact (almost 300% drop) on permeability reduction in Eagle Ford shale samples after huff and puff gas injection. Based on their results, 83% of total permeability is reduced owing to pore blockage and 17% reduction was due to adsorption mechanism.

### 4.4. Particle to pore size ratio

Experimental data adopted from Kord et al. [21] illustrates permeability reduction as a function of pore volume injected (Fig. 8). As it can be seen even after 0.5 pore volume injection, permeability reduction is close to 80%. If pore size and asphaltene particle size distributions (Fig. 9) are compared, it can be observed that particle to pore size ratio is close to one, which indicates that this significant reduction is because of pore blockage which is common for carbonate rock samples, consistent with our previous results.

Thus, it can be concluded that the relative difference between the size of deposited asphaltene particles and the pore size of a reservoir rock is a suitable measure to decide on which parameter is dominant in controlling asphaltene deposition in porous media. As illustrated in Fig. 10, if particle size is larger than deposited particle size, then surface deposition is the dominant factor on permeability reduction; pore throat plugging barely contributes to permeability loss. This typically happens in limestone. As the particle size increases and/or pore throat size reduces, one encounters the transition region; at this phase pore throat size and particle size are comparable close; both surface deposition and pore throat plugging contributes to permeability

reduction. This typically happens in sandstone. Finally, further increase in particle size results in the pore throat plugging becoming the dominant controlling parameter on permeability reduction; at this phase permeability reduction is steeper and sharper and this typically happens in carbonate [23]. There are no effective remedial actions for the pore throat dominant region. The only preventive method is not allowing precipitation to occur at the first place [14].

## 5. Conclusions

In this study, a new approach is examined for asphaltene deposition in the near wellbore region. The existing permeability impairment model (solely porosity-dependent models) was improved through incorporating interconnectivity loss due to pore blockage. The governing permeability impairment mechanism (either surface deposition or pore blockage) depends upon the ratio of asphaltene particle size to the pore throat size distribution:

1. Permeability reduction in the limestone samples studied here was due to surface deposition and the effect of pore blockage is negligible. This is because of the large ratio of pore throat to the particle size.
2. For the sandstone samples, both surface deposition and pore throat plugging mechanisms almost contribute equally to the permeability reduction.
3. For carbonate samples, the pore blockage is dominant. Thus, the sample experiences a rapid sharp permeability reduction.

## Acknowledgments

## References

[1] Behbahani TJ, Ghotbi C, Taghikhani V, Shahrabadi A. Experimental study and mathematical modeling of asphaltene deposition mechanism in core samples. Oil Gas Sci Technol – Revue d'IFP Energies Nouvelles 2013;70:1051–74. https://doi.org/10.2516/ogst/2013128.

[2] Bernabé Y, Li M, Maineult A. Permeability and pore connectivity: a new model based on network simulations. J Geophys Res Solid Earth 2010;115(B10).

[3] Boek ES, Wilson AD, Padding JT, Headen TF, Crawshaw JP. Multiscale simulation and experimental studies of asphaltene aggregation and deposition in capillary flow. Energy Fuels 2010;24(4):2361–8.

[4] Boek E, Fadili A, John Williams M, Padding J. Prediction of asphaltene deposition in porous media by systematic upscaling from a colloidal pore scale model to a deep bed filtration model. SPE 147539. Denver, Colorado, USA: SPE Annual Technical Conference and Exhibition held; 2011.

[5] Civan F. Scale effect on porosity and permeability: kinetics, model and correlation. AIChE J 2001;47:271–87.

[6] Civan F. Porous Media Transport Phenomena. Wiley; 2011. p. 15.

[7] Creek JL. Freedom of action in the state of asphaltenes: escape from conventional wisdom. Energy fuels 2005;19(4):1212–24.

[8] Dabir S, Dabir B, Moghanloo RG. A new approach to study deposition of heavy organic compounds in porous media. Fuel 2016;185:273–80.

[9] Daigle H. Application of critical path analysis for permeability prediction in natural porous media. Adv Water Resour 2016;96:43–54.

[10] Davudov D, Moghanloo RG, Flom J. Scaling analysis and its implication for asphaltene deposition in a Wellbore. Soc Petrol Eng 2017.

[11] Davudov D, Moghanloo RG. Impact of pore compressibility and connectivity loss on shale permeability. Int J Coal Geol 2018.

[12] Doyen PM. Permeability, conductivity, and pore geometry of sandstone. J Geophys Res Solid Earth 1988;93(B7):7729–40.

[13] Ghanbarian B, Hunt AG, Ewing RP, Skinner TE. Universal scaling of the formation factor in porous media derived by combining percolation and effective medium theories. Geophys Res Lett 2014;41(11):3884–90.

[14] Gonzalez D, Gonzales F, Pietrobon M, Haghshenas M, Shurn M, Mees A, Stewart C, Ogugbue C, Wilson A. "Strategies to Monitor and Mitigate Asphaltene Issues in the Production System of Gulf of Mexico Deepwater Subsea Development". J Petrol Technol 2016:92–4.

[15] Hamadou R, Khodja M, Kartout M, Jada A. Permeability reduction by asphaltenes and resins deposition in porous media. Fuel 2008;87:2178–85.

[16] Hematfar V, Ghazanfari MH, Bagheri MB. Modeling and optimization of asphaltene deposition in porous media using genetic algorithm technique. International Oil and Gas Conference and Exhibition in China. Society of Petroleum Engineers; 2010.

[17] Hunt AG. Applications of percolation theory to porous media with distributed local conductances. Adv Water Resour 2001;24(3):279–307.

[18] Flom Jonathan J, Moghanloo Rouzbeh G, Davudov Davud. Effects of hydrodynamic properties on asphaltene deposition in wellbore. J Petrol Sci Eng 2017;157:451–60. ISSN 0920-4105.

[19] Katz AJ, Thompson AH. "Quantitative Prediction of Permeability in Porous Rock". Phys. Rev. B 1986;34(11):8179–81.

[20] Katz AJ, Thompson AH. "Prediction of rock electrical conductivity from mercury injection measurements". J Geophys Res 1987;92(B1):599–607.

[21] Kord S, Miri R, Ayatollahi S, Escrochi M. Asphaltene deposition in carbonate rocks: experimental investigation and numerical simulation. Energy Fuels 2012;26(10):6186–99.

[22] Minssieux L. Core damage from crude asphaltene deposition. International Symposium on Oilfield Chemistry. Society of Petroleum Engineers; 1997.

[23] Moghanloo RG, Davudov D, Akita E. Formation damage by organic deposition. Formation Damage During Improved Oil Recovery 2018:243–73.

[24] Mousavi Dehghani SA, Vafaie Sefti M, Mirzayi B, Fasih M. Experimental investigation on asphaltene deposition in porous media during miscible gas injection. Iranian J Chem Chem Eng (IJCCE) 2007;26(4):39–48.

[25] Nasri Z, Dabir B. Network modeling of asphaltene deposition during two-phase flow in carbonate. J Petrol Sci Eng 2014;116:124–35.

[26] Revil A. The hydroelectric problem of porous rocks: thermodynamic approach and introduction of a percolation threshold. Geophys J Int 2002;151:944–9.

[27] Sahimi M. Applications of Percolation Theory. London: Taylor and Francis; 1994.

[28] Seifried, C. M., (2016) "Asphaltene Precipitation and Depostion from Crude Oil with CO2 and Hydrocarbons: Experimental Investigation and Numerical Simulation". Imperial College London, Department of Chemical Engineering. Sept. 2016.

[29] Shedid SA. Influences of asphaltene deposition on rock/fluid properties of low permeability carbonate reservoirs. SPE Middle East Oil Show. Society of Petroleum Engineers; 2001.

[30] Shen Z, Sheng JJ. Investigation of asphaltene deposition mechanisms during CO2 huff-n-puff injection in Eagle Ford shale. Pet Sci Technol 2017;35(20):1960–6. https://doi.org/10.1080/10916466.2017.1374403.

[31] Wang S. "Simulation of asphaltene deposition in petroleum reservoirs during primary oil recovery." PhD dissertation Norman, Oklahoma: University of Oklahoma; 2000

[32] Wang S, Civan F. "Productivity decline of vertical and horizontal wells by asphaltene deposition in petroleum reservoirs". SPE International Symposium on Oilfield Chemistry. Society of Petroleum Engineers; 2001.